

---

# Adversarial Feature Desensitization

---

**Pouya Bashivan**  
MILA, Université de Montréal  
Montreal, Canada  
bashivap@mila.quebec

**Blake Richards**  
MILA, McGill University  
Montreal, Canada  
blake.richards@mila.quebec

**Irina Rish**  
MILA, Université de Montréal  
Montreal, Canada  
irina.rish@mila.quebec

## Abstract

Deep neural networks can now perform many tasks that were once thought to be only feasible for humans. Unfortunately, while reaching impressive performance under standard settings, such networks are known to be susceptible to adversarial attacks – slight but carefully constructed perturbations of the inputs which drastically decrease the network performance and reduce their trustworthiness. Here we propose to improve network robustness to input perturbations via an adversarial training procedure which we call *Adversarial Feature Desensitization (AFD)*. We augment the normal supervised training with an adversarial game between the embedding network and an additional adversarial decoder which is trained to discriminate between the clean and perturbed inputs from their high-level embeddings. Our theoretical and empirical evidence acknowledges the effectiveness of this approach in learning robust features on MNIST, CIFAR10, and CIFAR100 datasets – substantially improving the state-of-the-art in robust classification against previously observed adversarial attacks. More importantly, we demonstrate that AFD has better generalization ability than previous methods, as the learned features maintain their robustness against a large range of perturbations, including perturbations not seen during training. These results indicate that reducing feature sensitivity using adversarial training is a promising approach for ameliorating the problem of adversarial attacks in deep neural networks.

## 1 Introduction

Recent progress in deep learning has allowed neural network models to achieve a near human-level performance across a range of complex tasks [16, 31, 39, 46]. However, while the number of applications of deep learning is growing fast, these systems are often not very robust. In particular, their vulnerability to *adversarial attacks* [44] has critically diminished the public trust in these systems. Adversarial attacks are small but precise perturbations made to the inputs of a system, resulting in high-confidence predictions which are critically divergent from human judgement.

It has been shown that many adversarial perturbations that are often small in magnitude lead to large deviations in the high-level features of deep neural networks [50]. In addition, previous work demonstrated that adversarial patterns often rely on specific learned features which generalize even on large datasets such as Imagenet [17]. However, these features are highly sensitive to input changes, yielding a potential vulnerability that can be exploited by adversarial attacks. While humans can

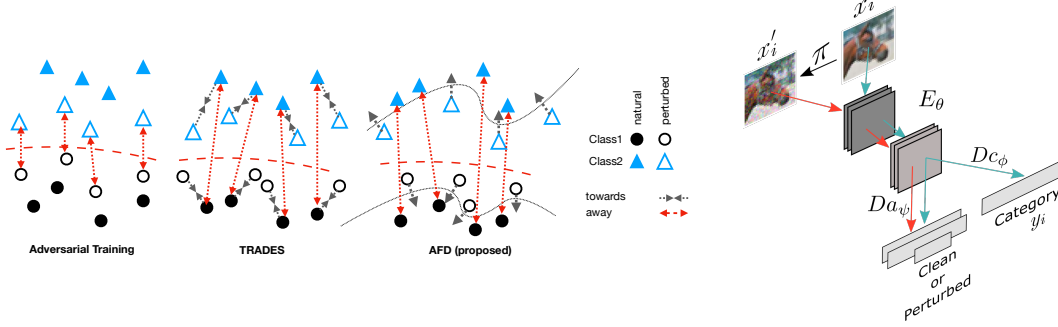


Figure 1: Overview of the proposed approach (left) visual comparison of different adversarial robustness methods. Adversarial training [26], TRADES [52], and AFD. The dotted line corresponds to the decision boundary of the adversarial decoder (right) schematic of AFD paradigm.

also experience altered perception in response to particular visual patterns (e.g., *visual illusions*<sup>1</sup>), they are seemingly insensitive to this particular class of perturbations, and often unaware of the subtle image changes resulting from adversarial attacks. This in turn suggests that current artificial neural networks rely on visual features that are still considerably different from those giving rise to perception in primates (and, particularly, in humans) – even despite many recent studies highlighting their remarkable similarities [49, 20, 2]. It is therefore reasonable to hypothesize that a deep network may become more robust to such adversarial attacks if the corresponding higher-level representations (features, embeddings) are more robust to input perturbations, similar to those used by our brains. One way to approach the question of feature/embedding robustness is to use a relatively simple classifier (e.g. a linear transformation) that produces predictions based on such embedding — if the embedding is robust then the predictions from the simple classifier would consequently be robust too. We use this approach below to develop our technique for improved embedding robustness.

Formally, for a given embedding function  $E$  (for example, the activations before the last linear layer in a deep neural network), we define the embedding sensitivity  $\epsilon_e$  as the maximum change in the embedding given input perturbations  $\delta$  of maximum size  $\epsilon_i$ :

$$\forall x \in \mathcal{X}, \|\delta\| \leq \epsilon_i; \max_{\delta} \|E(x) - E(x + \delta)\| \leq \epsilon_e \quad (1)$$

Following the above reasoning, we wish to discourage the embedding from learning over-sensitive features ( $\epsilon_e \gg 0$ ) because *a representation devoid of over-sensitive features will only gradually change in response to input variations and will not allow drastic changes in the category judgments derived from it*. However in practice, achieving full embedding robustness under equation (1) might be difficult. On the other hand, from the point of view of category judgements, some embedding sensitivity could still be acceptable as long as it would not lead to drastic changes in the category judgements. Such that, given a decoding function  $Dc$ :

$$\forall x \in \mathcal{X}, \|\delta\| \leq \epsilon_i : \max_{\delta} \|Dc(E(x)) - Dc(E(x + \delta))\| \leq K\delta \quad (2)$$

which provides a formulation of the problem that is similar to the Lipschitz continuity and where we desire  $K$  to be small.

In principal, drastic changes in category judgements could occur under at least one of the following two conditions: i) when  $K$  is relatively small but the class manifolds are close to each other in the embedding space; ii) when class manifolds are reasonably apart but points in the embedding space can have gradients that are large enough to allow the feature values to essentially *teleport* from the manifold of one class to another (i.e. when  $K \gg 0$ ).

Many prior work on adversarial robustness have tackled the robust classification problem by pushing the embedding of training samples from different categories farther from the decision boundary [26, 18, 52], which has been shown to lead to significant improvement in adversarial robustness given a specific perturbation. For example, in Adversarial Training procedure [26], network is trained

<sup>1</sup><https://michaelbach.de/ot/>

to optimize the classification loss on the perturbed inputs or in combination with clean inputs. Or another recent approach called TRADES [52] augments the classification loss on clean inputs with an auxiliary term that matches the assigned labels to clean and perturbed inputs (Figure-1). However neither of these methods address the potential issues that may rise under the second condition mentioned above (i.e. when the embedding could exhibit sharp changes in response to small input perturbations that could still lead to crossing the classification boundary). On the other hand, several other works attempted to improve robustness by enhancing the flatness of the classification loss [47, 34], which demonstrated that this approach will also lead to more robust performance against white-box attacks.

Here, instead of focusing on robust classification, we turned our attention to robustness of learned features from which the categories are inferred (e.g. using a simple linear classifier). Ideally, we want the learned embeddings to remain stable in the presence of small adversarial or non-adversarial perturbations. We propose to improve the robustness of network embeddings to adversarial perturbations via an adversarial game between two agents. In this setup, the first adversarial agent (i.e. the attacker) searches for performance-degrading perturbations given the embedding function. On the other hand, the second agent uses a decoder function to discriminate between the clean and perturbed inputs from their high-level embeddings. The parameters of the embedding and (adversarial) decoding functions are then tuned via an adversarial game between the two (Figure-1). This paradigm is similar to the adversarial learning paradigm widely used in image generation and transformation [14, 19, 54], unsupervised and semi-supervised learning [30], video prediction [27, 23], domain adaptation [13, 45], active learning [40], and continual learning [12].

In summary, our main contributions are as follows:

- We introduce a method to improve the robustness of learned features in an embedding network through an adversarial game between the embedding network and a secondary decoding network.
- We theoretically demonstrate that under some assumptions on the nature of the adversarial attacker, this approach leads to a flat likelihood function in the vicinity of training samples.
- We empirically confirm that the proposed feature desensitization approach leads to learning a sparse and robust set of high-level features and consequently a more stable classifier.

## 2 Methods

Let  $E(x) : \mathbb{R}^{N_i} \rightarrow \mathbb{R}^{N_e}$  be an embedding of the input  $x$  with  $N_i$  inputs and  $N_e$  embeddings, and  $D_c : \mathbb{R}^{N_e} \rightarrow \mathbb{R}^{N_c}$  be a linear function that when applied on the embedding  $E(x)$  outputs the likelihood of possible labels given the input  $x$ :  $\hat{l}_i(x) = \text{softmax}(D_c(E(x))), i \in \{1, \dots, N_c\}$ . Let  $\pi(x, \epsilon)$  be a perturbation which operates on input  $x$ :

$$\forall x \in \mathcal{X} : \pi(x, \epsilon) = x' \in \mathcal{B}(x, \epsilon); \mathcal{B}(x, \epsilon) = \{x' \in \mathcal{X} : \|x' - x\| < \epsilon\} \quad (3)$$

which finds perturbations within the  $\epsilon$  neighborhood of input  $x$  such that:

$$\text{argmax}_i \hat{l}_i(x) \neq \text{argmax}_i \hat{l}_i(x') \quad (4)$$

Given any model, there are at least two conditions under which a perturbation method  $\pi$  could drastically increase the likelihood of the non-target class. i) there are short paths from points on the manifold of one class to another; ii) there are points on the manifold of one class with large gradients in the direction of another class. Notably, under the second condition, it is possible for the manifolds of two classes to be far from each other but still the underlying embedding space to be non-robust.

Ideally we want a network to learn an embedding that remains stable in the presence of any small perturbations while considering both of the above possible situations. Consequently, to learn such an embedding, one needs to not only increase the distance between manifolds of different classes, but also to *reduce the magnitude of gradients from points on the manifold of each class in the direction of other classes*.

In that regard, several prior studies have explored different approaches towards increasing the distance between class manifolds [26, 52]. These approaches lead to substantial increase in robust performance against adversarial perturbations. However, they commonly suffer from sudden dives in performance

with slight increments to the strength of perturbations or by being exposed to a different class of perturbations [38, 41].

We posit that the landscape of gradients in the learned embedding space is equally important for the robustness of model’s performance against adversarial perturbations and hypothesize that the failure of previous approaches in generalizing the robust performance to higher perturbation degrees may be (at least partly) due to the potentially large likelihood gradients that remain unconstrained. We propose an adversarial learning procedure to reduce the sensitivity of the learned embedding with respect to the input. Algorithm 1 summarizes the proposed approach. The training procedure involves three loss functions that are optimized sequentially. First, parameters of the embedding  $E_\theta$  and category decoder  $Dc_\phi$  are tuned to minimize the categorization softmax entropy loss. Second, parameters of the adversarial decoder  $Da_\psi$  are tuned to minimize the cross-entropy loss associated with discriminating natural and perturbed inputs conditioned on the natural labels. Lastly, parameters of the embedding  $E_\theta$  are adversarially tuned to maximize the cross-entropy from the second step. The adversarial training framework is similar to that used in training conditional GANs, in which  $E$  and  $Da$  networks play a two-player minimax game with value function  $V(E, Da)$ :

$$V(E, Da) = \mathbb{E}_{p(y)} [\mathbb{E}_{p(x|y)} [\mathcal{S}(-Da(E(x), y))]] + \mathbb{E}_{q(y)} [\mathbb{E}_{q(x|y)} [\mathcal{S}(Da(E(x), y))]] \quad (5)$$

where  $p$  and  $q$  correspond to natural and perturbed distributions, and  $\mathcal{S}$  denotes the softplus function. Following the logic presented in [14, 7] we reason that the global minimum of the adversarial training criterion  $V(E, Da)$  is achieved if and only if  $p = q$  and the embedding of natural and perturbed images conditioned on the class label are indistinguishable from each other:

$$P(E(x), y) = P(E(x'), y) \quad (6)$$

If this is the case, then a Bayes optimal classifier will achieve the same error rate on the perturbed inputs as it will on the natural inputs. We use this fact below to prove that when  $V(E, Da)$  is at the global minimum, the partial derivatives of the linear output with respect to the input in the perturbation direction are zero, i.e. the gradient is flat in the direction of the other classes.

**Theorem 1.** *Given an embedding function  $E(x)$ , class-likelihood functions  $Dc_i, i \in \{1, \dots, K\}$ :  $\hat{l}_i(x) = \text{softmax}(Dc_i(E(x)))$ , a perturbation function  $\pi(x) = x - \frac{\partial \hat{l}_t}{\partial x}$  where  $t$  denotes the target (true) class index, if the adversarial optimization of embedding and discriminator functions  $E$  and  $Da$  converges to its global minimum of the training criterion, then  $\frac{\partial \hat{l}_t}{\partial x}|_{x=x_i} = 0$ .*

*Proof.* Assume  $Dc_i, i \in \{1, \dots, K\}$  is a set of differentiable functions that implement the Bayes optimal classifier from the  $E(x)$  embedding.

$$\begin{aligned} \hat{y} &= \text{argmax}_i \hat{l}_i \\ \hat{l}_i &= P(y_i|x) = \text{softmax}(Dc_i(E(x))), y_i \in \{1, \dots, K\} \end{aligned} \quad (7)$$

Assuming that the adversarial training of  $E$  and  $Da$  converge to the global minimum, we have:

$$\forall x \in \mathcal{X}, y \in \mathcal{Y} : P(E(x), y) = P(E(\pi(x)), y) \quad (8)$$

Following from Bayes rule we have:

$$P(y_i = t|E(x_i))P(E(x_i)) = P(y_i = t|E(x_i - \delta))P(E(x_i - \delta)), \delta = \frac{\partial \hat{l}_t}{\partial x} \Big|_{x=x_i} \quad (9)$$

From equation 8, the marginal distributions  $P(E(x_i))$  and  $P(E(x_i - \delta))$  should be equal which leads to:

$$P(y_i = t|E(x_i)) = P(y_i = t|E(x_i - \delta)) \quad (10)$$

which can only be true if  $\frac{\partial \hat{l}_t}{\partial x}|_{x=x_i} = 0$ .  $\square$

---

**Algorithm 1:** AFD training procedure

---

**Input:** Perturbation  $\pi$ , batch size  $m$ , optimizer  $\mathcal{O}$ , encoding network  $E_\theta$ , adversarial decoder network  $Da_\psi$ , category decoder network  $Dc_\phi$ , softplus function  $\mathcal{S}$ .

Read mini-batch  $B = \{(x_1, y_1), \dots, (x_m, y_m)\}$

**repeat**

$$\begin{aligned} x' &\leftarrow \pi(x, E_\theta, Dc_\phi) \\ \mathcal{L}_{EDc} &= -\frac{1}{m} \sum_{i=1}^m \log(\text{softmax}(-Dc_\phi(E_\theta(x_i)), y_i)) \\ \mathcal{L}_{Da} &= \frac{1}{m} \sum_{i=1}^m [\mathcal{S}(-Da_\psi(E_\theta(x_i))) + \mathcal{S}(Da_\psi(E_\theta(x'_i)))] \\ \mathcal{L}_E &= \frac{1}{m} \sum_{i=1}^m \mathcal{S}(-Da_\psi(E_\theta(x'_i))) \\ \theta, \phi &\leftarrow \mathcal{O}(\theta, \phi, \nabla_{\theta, \phi} \mathcal{L}_{EDc}) \\ \psi &\leftarrow \mathcal{O}(\psi, \nabla_\psi \mathcal{L}_{Da}) \\ \theta &\leftarrow \mathcal{O}(\theta, \nabla_\theta \mathcal{L}_E) \end{aligned}$$

**until** training converged;

---

While the assumption of convergence to global optimum is a strong assumption, in practice, it is possible to derive a bound on the classifier’s robust error in terms of its error on clean inputs and a divergence measure between the clean and perturbed embeddings (see 8.3 in the appendix).

### 3 Experiments

#### 3.1 Adversarial perturbations

We used a range of adversarial perturbations in our experiments, using existing implementations in the Foolbox [35] and Advtorch [9] packages. We validated the models against Projected Gradient Descent (PGD) [26] ( $L_\infty, L_2, L_1$ ), Fast Gradient Sign Method (FGSM) [15], Momentum Iterative Method (MIM) [10], Decoupled Direction and Norm (DDN) [36], Deepfool [32], and C&W [5] perturbations. For each perturbation, we swept the  $\epsilon$  value across a wide range and validated different models on each. Specific settings used for each perturbation are listed in Table-A3.

#### 3.2 Adversarial robustness

We validated our approach on learning robust visual embeddings on the MNIST[22], CIFAR10, and CIFAR100[21] datasets. We used projected gradient descent with  $L_\infty$  constraint to perturb the inputs during training.  $\epsilon$  was set to 0.3 and 0.031 for MNIST and CIFAR datasets respectively. We used the activations before the last linear layer as the high-level embedding produced by the network. In all experiments, the adversarial decoder network ( $D_a$ ) consisted of three fully connected layers with Leaky ReLU nonlinearity followed by a projection discriminator layer that incorporated the labels into the adversarial decoder through a dot product operation [29]. The number of hidden units in all layers were equal (200 for MNIST and 512 for CIFAR10). We used spectral normalization [28] on all layers of  $D_a$ . Further details of training for each experiment are listed in Table-A2. We used our own re-implementation of adversarial training (AT) method [26] and the official code for TRADES<sup>2</sup> [52] and denoted these results with † in the tables.

**Adversarial robustness against observed attack** We first evaluated our approach against the same class and strength of attack that was used during training. Table-1 compares the robust classification performance of our proposed approach against PGD  $L_\infty$  (with similar setting as was used during training) and FGSM attacks. Training LeNet with AFD was unstable leading to frequent crashing of adversarial decoder accuracy despite our extensive hyperparameter search. For this reason, we conducted our MNIST experiments using a very shallow ResNet architecture which we call ResNet5. This architecture consisted of only one convolution, one ResNet block, and a fully connected layer with a total depth of 5 layers (Table-A1). AFD-trained ResNet5 was less robust compared to AT against PGD- $L_\infty$  and FGSM with default strength. On the other hand, on CIFAR10 and CIFAR100 datasets, ResNet18 network trained with AFD performed much higher than all other methods against both white-box and black-box attacks.

---

<sup>2</sup><https://github.com/yaodongyu/TRADES.git>

Table 1: Accuracy against different perturbations and methods on MNIST, CIFAR10, and CIFAR100 datasets. Both PGD $_{L_\infty}$  and FGSM perturbations were constrained by  $\epsilon = 0.3$  for MNIST and  $\epsilon = \frac{8}{255}$  for CIFAR10 and CIFAR100 datasets. † indicates replicated results using our reimplementation or official code. NT: natural training; AT: adversarial training; AFD: adversarial feature desensitization; WB: white-box attack; BB: black-box attack. Numbers reported with  $\mu \pm \sigma$  denote mean and std values over three independent runs with different random initialization. \* RST[6] additionally uses 500K unlabeled images during training.

Method	Dataset	Network	Clean	PGD $_{L_\infty}$ (WB)	FGSM (WB)	PGD $_{L_\infty}$ (BB)	FGSM (BB)
NT†	MNIST	LeNet	98.88	0	0.45	0	0.44
AT[26]		LeNet	98.8	93.2	95.6	96.0	96.8
TRADES[52]		LeNet	<b>99.48</b>	<b>96.07</b>	-	-	-
ATES[41]		LeNet	99.11	94.04	-	-	-
ABS[38]		LeNet	99.0	13	34	-	-
NT†		RN5	98.81±0.03	2.03±0.23	9.72±0.01	2.08±0.16	9.74±0.0
AT[26]†		RN5	99.15±0.07	94.98±0.09	<b>97.1±0.11</b>	<b>98.96±0.05</b>	<b>98.92±0.08</b>
TRADES[52]†		RN5	97.72±0.11	89.87±0.87	95.18±1.02	96.88±0.4	95.08±1.49
AFD		RN5	98.49±0.16	92.75±0.32	95.95±0.46	98.11±0.25	97.97±0.25
NT†	CIFAR10	RN18	<b>95.40</b>	0.12	47.79	12.00	54.65
AT[26]		RN18	87.3	45.8	56.1	86.0	<b>85.6</b>
AT[26]†		RN18	83.58	41.05	50.12	83.20	82.88
TRADES[52]		RN18	84.92	56.61	-	-	-
TRADES[52]†		RN18	82.22	52.30	58.16	80.36	79.69
ATES[41]		WRN-34-10	86.84	55.06	-	-	-
RLFAT[43]		WRN-32-10	82.72	58.75	-	-	-
RST+[47, 6]*		WRN-34-10	89.82	64.86	69.60	<b>88.77</b>	<b>87.61</b>
LLR[34]		WRN-28-8	86.83	52.99	-	-	-
AFD		RN18	87.83	<b>72.45</b>	<b>76.43</b>	86.28	85.06
NT†	CIFAR100	RN18	<b>76.12</b>	0.01	9.67	1.55	15.43
AT[26]†		RN18	55.78	20.39	25.09	53.83	53.25
TRADES[52]†		RN18	55.48	27.36	30.46	54.13	53.16
RLFAT[43]		WRN-32-10	56.70	31.99	-	-	-
AFD		RN18	62.54	<b>49.89</b>	<b>51.36</b>	<b>58.95</b>	<b>56.59</b>

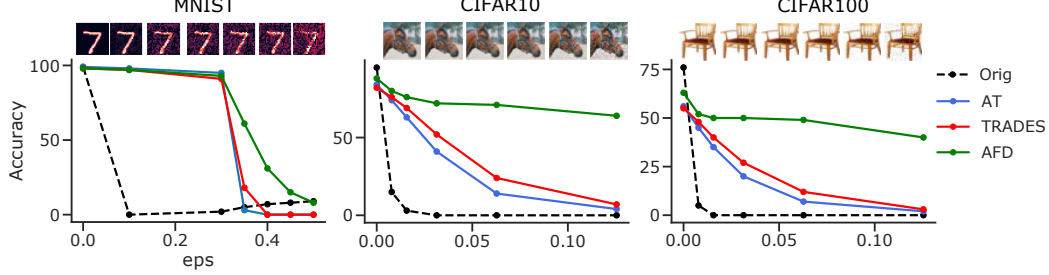


Figure 2: Robust classification performance of different methods against various degrees of PGD- $L_\infty$  attack on different datasets.

**Robust classification against stronger and unseen attacks** We also tested the network robustness against higher degrees of the same attack used during training as well as to a suite of other (unobserved) attacks. We found that the AFD-trained networks continued to perform relatively well against white-box attacks even for very large perturbations – while performance of other methods went down to zero relatively quickly (Figures-2,A2,A3,A4). The AFD-trained network also performed remarkably well against most other perturbation methods that were not observed during training. To compare different models considering both attack types and perturbation strength, we computed the area-under-the-curve (AUC) for a range of epsilons for each attack and each approach. Table-2 summarizes these values for our approach and two alternative approaches (adversarial training and TRADES).

**Embedding Stability** We compared the robustness of the learned embedding derived from training the same architecture using different methods. For that we measured the normalized sensitivity of the embeddings in each network as  $\frac{\|E(x) - E(x')\|_2}{\|E(x)\|_2}$ . For all three datasets we found that AFD-trained network learns high-level features that are more robust against input perturbations as measured by the normalized L2 distance between clean and perturbed embeddings (Figures-A1,A6,A7,A8).

Table 2: AUC measures for different perturbations and methods on MNIST, CIFAR10, and CIFAR100 datasets. AUC values are normalized to have a maximum allowable value of 1. Evaluations on AT and TRADES were made on networks trained using reimplemented or official code.

Dataset	Model	PGD <sub>L<sub>∞</sub></sub>	PGD <sub>L<sub>2</sub></sub>	PGD <sub>L<sub>1</sub></sub>	FGSM	MIM	DDN	DeepFool	C&W
MNIST	NT (RN5)	0.13	0.10	0.08	0.18	0.10	0.05	0.05	0.23
	AT (RN5)	0.64	0.22	0.20	0.67	0.64	0.45	<b>0.42</b>	<b>0.84</b>
	TRADES (RN5)	0.63	0.21	0.14	0.69	<b>0.65</b>	0.45	0.40	<b>0.84</b>
	AFD (RN5)	<b>0.73</b>	<b>0.33</b>	<b>0.28</b>	<b>0.73</b>	0.64	<b>0.46</b>	0.40	0.76
CIFAR10	NT (RN18)	0.04	0.02	0.03	0.25	0.04	0.06	0.06	0.10
	AT (RN18)	0.27	0.05	0.07	0.31	0.29	0.06	0.18	0.26
	TRADES (RN18)	0.34	0.06	0.08	0.33	0.36	0.06	<b>0.25</b>	<b>0.32</b>
	AFD (RN18)	<b>0.71</b>	<b>0.32</b>	<b>0.53</b>	<b>0.74</b>	<b>0.73</b>	<b>0.34</b>	0.15	0.25
CIFAR100	NT (RN18)	0.03	0.02	0.01	0.06	0.03	0.05	0.01	0.08
	AT (RN18)	0.15	0.03	0.04	0.12	0.15	0.04	0.09	0.14
	TRADES (RN18)	0.19	0.04	0.05	0.15	0.18	0.04	<b>0.11</b>	<b>0.17</b>
	AFD (RN18)	<b>0.48</b>	<b>0.18</b>	<b>0.33</b>	<b>0.50</b>	<b>0.50</b>	<b>0.15</b>	0.07	0.11

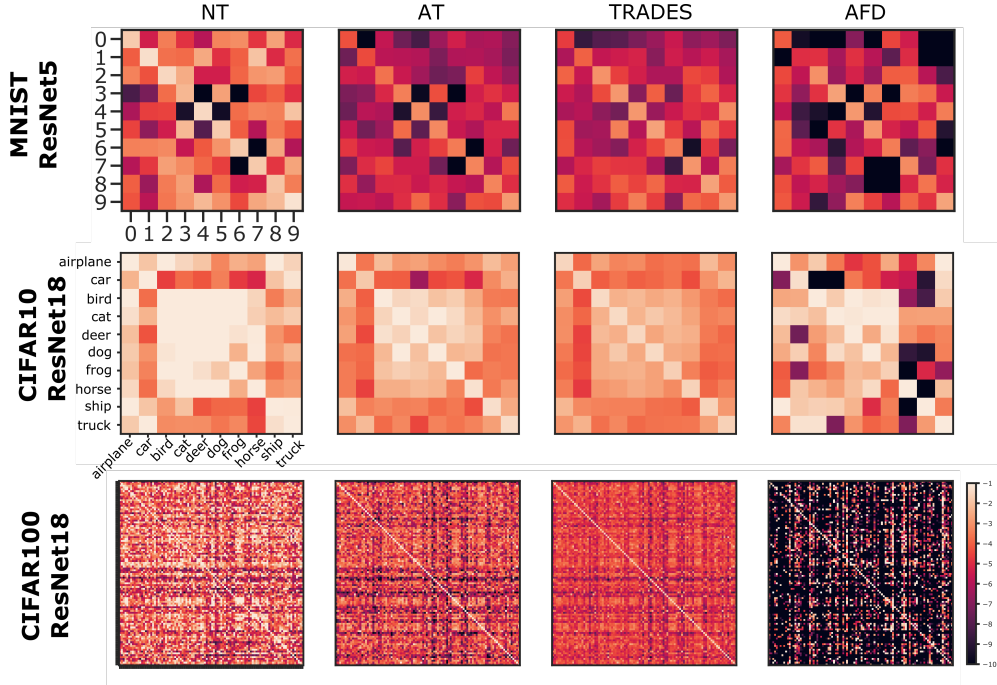


Figure 3: Logarithm of the average gradient magnitudes of class likelihoods with respect to input, evaluated at samples within the test set of each dataset ( $\log(\mathbb{E}_{x \sim \mathcal{X}}(\frac{\partial \hat{y}_t}{\partial x} |_{x=x_i}))$ ). For each matrix, rows correspond to target (true) labels and columns correspond to non-target labels.

**Learning a sparse embedding** We compared the number of embedding dimensions learned by applying different methods on the same architecture using two measures. i) number of non-zero units over the test set within each dataset and ii) number of PCA dimensions that explains more than 99% of the variance in the embedding computed over the test-set of each dataset. We found that the same network architecture when trained with AFD method gave rise to a much sparser and lower dimensional embedding space (Table-A5). The embedding spaces learned with AFD on MNIST, CIFAR10, and CIFAR100 datasets had only 4, 7, and 88 principal components respectively.

**Gradient landscape** To empirically validate our proposed theorem, we computed the average gradient of each predicted class with respect to the input across samples within the test set of each dataset ( $\|\nabla_x \hat{l}_i\|, i \in 1, \dots, K$ ). We found that, on all datasets, the magnitude of gradients in the direction of most non-target classes were much smaller for AFD-trained network compared to other tested

methods (Figure-3). This confirms that AFD stabilizes the embedding in a way that significantly reduces the gradients towards most non-target classes.

**Matching vs. Indiscrimination** We also ran additional experiments on the MNIST dataset in which we added a regularization term to the classification loss to minimize the  $L_2$  distance between the clean and perturbed embeddings. We observed that although this augmented loss improved the network robustness against different white box attacks, it showed only weak generalization to higher strength and other unseen perturbations (Figure-A5). This result suggests that enforcing a distributional form of feature desensitization (e.g. AFD) may lead to robust behavior over a larger range of perturbations compared to the case where feature stability is directly enforced through an  $L_p$  norm measure.

**Non-obfuscated gradients** Recent literature have pointed out that many defense methods against adversarial perturbations could drive the network into a regime called *obfuscated gradients* in which the network appears to be robust against common iterative adversarial attacks but could easily be broken using black-box or alternative attacks that do not rely on exact gradients [33, 1]. We believe that our results are not due to obfuscated gradients for several reasons. i) For most perturbations, the model performance continues to decrease with increased epsilon (Figures-A2,A3,A4); ii) The iterative perturbations were consistently more successful than single-step ones (Table-1); iii) Black-box attacks were significantly less successful than white-box attacks (Table-1); iv) The AFD-trained model performed similar or better than alternate methods against the Boundary attack [4] – an attack which does not rely on the network gradients (Table-A4).

## 4 Related Work

There is an extensive literature on mitigating susceptibility to adversarial perturbations. Adversarial training [26] is one of the earliest successful attempts to improve robustness of the learned representations to potential perturbations to the input pattern by solving a "saddle point" problem composed of an inner and outer adversarial optimization. A number of other works suggest additional losses instead of direct training on the perturbed inputs. TRADES [52] adds a regularization term to the cross-entropy loss which penalizes the network for assigning different labels to natural images and their corresponding perturbed images. [34] proposed an additional regularization term (local linearity regularizer) that encourages the classification loss to behave linearly around the training examples. [47] proposed to regularize the flatness of the loss to improve adversarial robustness.

Our work is closely related to the domain adaptation literature in which adversarial optimization has recently gained much attention [13, 24, 45]. From this viewpoint one could consider the clean and perturbed inputs as two distinct domains for which a network aims to learn an invariant feature set. Although in our setting, i) the perturbed domain continuously evolves while the parameters of the embedding network are tuned; ii) unlike the usual setting in domain-adaptation problems, here we have access to the labels associated with samples from the perturbed (target) domain. Despite this, [42] regularized the network to have similar logit values in response to clean and perturbed inputs and showed that this additional term leads to better robust generalization to unseen perturbations. Related to this, Adversarial Logit Pairing [18] increases robustness by directly matching the logits for clean and adversarial inputs.

Another line of work is on developing certified defenses which consist of methods with provable bounds over which the network is *certified* to operate robustly [53, 51, 8]. While these approaches provide a sense of guarantee about the proposed defenses, they are usually prohibitively expensive to train, drastically reduce the performance of the network on natural images, and the empirical robustness gained against standard attacks are low.

## 5 Discussion

We proposed a method to decrease the sensitivity of learned embeddings in neural networks using adversarial optimization. Decreasing the input-sensitivity of features has long been desired in training neural networks [11] and has been suggested as a way to improve adversarial robustness [37]. Our results show that AFD can be used to reduce the sensitivity of network features to input perturbations and to improve robustness against a family of adversarial attacks. We believe that these results could further be improved by i) using larger neural networks such as wider or deeper networks as is shown in recent work [48, 26]; ii) by applying the adversarial learning paradigm on multiple feature layers



of the network; iii) by combining AFD with other methods like adversarial training [26] or TRADES [52].

## 6 Broader Impact

As the application of deep neural networks becomes more common in everyday life, security and dependability of these networks becomes more crucial. While these networks excel at performing many complicated tasks under standard settings, they often are criticized for their lack of reliability under broader settings. One of the main points of criticism of today’s artificial neural networks is on their vulnerability to adversarial patterns – slight but carefully constructed perturbations of the inputs which drastically decrease the network performance.

Our work presented here proposes a new way of addressing this important issue. Our approach could be used to improve the robustness of learned representation in an artificial neural network and as shown lead to a recognition behavior that is more aligned with the human judgement. More broadly, the ability to learn robust representations and behaviors is highly desired in a wide range of applications and disciplines including perception, control, and reasoning and we expect the presented work to influence the future studies in these areas.

## 7 Acknowledgements

We would like to thank Isabela Albuquerque, Joao Monteiro, Alexia Jolicoeur-Martineau, and Mojtaba Faramarzi for their valuable comments on the manuscript. Pouya Bashivan is partially supported by the Unifying AI and Neuroscience – Québec (UNIQUE) Postdoctoral fellowship.

## References

- [1] Anish Athalye, Nicholas Carlini, and David Wagner. Obfuscated gradients give a false sense of security: Circumventing defenses to adversarial examples. *35th International Conference on Machine Learning, ICML 2018*, 1:436–448, 2018.
- [2] Pouya Bashivan, Kohitij Kar, and James J DiCarlo. Neural Population Control via Deep Image Synthesis. *Science*, 364(6439), 2019.
- [3] Shai Ben-David, John Blitzer, Koby Crammer, Alex Kulesza, Fernando Pereira, and Jennifer Wortman Vaughan. A theory of learning from different domains. *Machine Learning*, 79(1-2):151–175, 2010.
- [4] Wieland Brendel, Jonas Rauber, and Matthias Bethge. Decision-based adversarial attacks: Reliable attacks against black-box machine learning models. *ICLR*, pages 1–12, 2018.
- [5] Nicholas Carlini and David Wagner. Towards Evaluating the Robustness of Neural Networks. *Proceedings - IEEE Symposium on Security and Privacy*, pages 39–57, 2017.
- [6] Yair Carmon, Aditi Raghunathan, Ludwig Schmidt, John C Duchi, and Percy S Liang. Unlabeled data improves adversarial robustness. In *Advances in Neural Information Processing Systems*, pages 11190–11201, 2019.
- [7] Grigorios G Chrysos, Jean Kossaifi, and Stefanos Zafeiriou. Robust conditional generative adversarial networks. *ICLR*, pages 1–27, 2019.
- [8] Jeremy Cohen, Elan Rosenfeld, and J. Zico Kolter. Certified adversarial robustness via randomized smoothing. *36th International Conference on Machine Learning, ICML 2019*, 2019-June:2323–2356, 2019.
- [9] Gavin Weiguang Ding, Luyu Wang, and Xiaomeng Jin. AdverTorch v0.1: An adversarial robustness toolbox based on pytorch. *arXiv preprint arXiv:1902.07623*, 2019.
- [10] Yinpeng Dong, Fangzhou Liao, Tianyu Pang, Hang Su, Jun Zhu, Xiaolin Hu, and Jianguo Li. Boosting Adversarial Attacks with Momentum. *Proceedings of the IEEE Computer Society Conference on Computer Vision and Pattern Recognition*, pages 9185–9193, 2018.
- [11] Harris Drucker and Yann Le Cun. Improving generalization performance using double back-propagation. *IEEE Transactions on Neural Networks*, 3(6):991–997, 1992.

- [12] Sayna Ebrahimi, Franziska Meier, Roberto Calandra, Trevor Darrell, and Marcus Rohrbach. Adversarial continual learning. *arXiv preprint arXiv:2003.09553*, 2020.
- [13] Yaroslav Ganin and Victor Lempitsky. Unsupervised domain adaptation by backpropagation. *32nd International Conference on Machine Learning, ICML 2015*, 2(i):1180–1189, 2015.
- [14] Ian Goodfellow, Jean Pouget-Abadie, Mehdi Mirza, Bing Xu, David Warde-Farley, Sherjil Ozair, Aaron Courville, and Yoshua Bengio. Generative adversarial nets. In *Advances in neural information processing systems*, pages 2672–2680, 2014.
- [15] Ian J Goodfellow, Jonathon Shlens, and Christian Szegedy. Explaining and harnessing adversarial examples. *arXiv preprint arXiv:1412.6572*, 2014.
- [16] Kaiming He, Xiangyu Zhang, Shaoqing Ren, and Jian Sun. Deep residual learning for image recognition. In *Proceedings of the IEEE conference on computer vision and pattern recognition*, pages 770–778, 2016.
- [17] Andrew Ilyas, Shibani Santurkar, Dimitris Tsipras, Logan Engstrom, Brandon Tran, and Aleksander Madry. Adversarial examples are not bugs, they are features. In *Advances in Neural Information Processing Systems*, pages 125–136, 2019.
- [18] Harini Kannan, Alexey Kurakin, and Ian Goodfellow. Adversarial logit pairing. *arXiv preprint arXiv:1803.06373*, 2018.
- [19] Tero Karras, Samuli Laine, and Timo Aila. A style-based generator architecture for generative adversarial networks. In *Proceedings of the IEEE Conference on Computer Vision and Pattern Recognition*, pages 4401–4410, 2019.
- [20] Seyed Mahdi Khaligh-Razavi and Nikolaus Kriegeskorte. Deep Supervised, but Not Unsupervised, Models May Explain IT Cortical Representation. *PLoS Computational Biology*, 10(11), 2014.
- [21] Alex Krizhevsky, Geoffrey Hinton, et al. Learning multiple layers of features from tiny images. 2009.
- [22] Yann LeCun, Léon Bottou, Yoshua Bengio, and Patrick Haffner. Gradient-based learning applied to document recognition. *Proceedings of the IEEE*, 86(11):2278–2324, 1998.
- [23] Alex X Lee, Richard Zhang, Frederik Ebert, Pieter Abbeel, Chelsea Finn, and Sergey Levine. Stochastic adversarial video prediction. *arXiv preprint arXiv:1804.01523*, 2018.
- [24] Hong Liu, Mingsheng Long, Jianmin Wang, and Michael Jordan. Transferable Adversarial Training: A General Approach to Adapting Deep Classifiers. *International Conference on Machine Learning*, pages 4013–4022, 2019.
- [25] Laurens van der Maaten and Geoffrey Hinton. Visualizing data using t-sne. *Journal of machine learning research*, 9(Nov):2579–2605, 2008.
- [26] Aleksander Madry, Aleksandar Makelov, Ludwig Schmidt, Dimitris Tsipras, and Adrian Vladu. Towards deep learning models resistant to adversarial attacks. *arXiv preprint arXiv:1706.06083*, 2017.
- [27] Michael Mathieu, Camille Couprie, and Yann LeCun. Deep multi-scale video prediction beyond mean square error. *arXiv preprint arXiv:1511.05440*, 2015.
- [28] Takeru Miyato, Toshiki Kataoka, Koyama Masanori, and Yoshida Yuichi. Spectral normalization for generative adversarial networks. *ICLR*, 2018.
- [29] Takeru Miyato and Masanori Koyama. cgans with projection discriminator. *arXiv preprint arXiv:1802.05637*, 2018.
- [30] Takeru Miyato, Shin Ichi Maeda, Shin Ishii, and Masanori Koyama. Virtual Adversarial Training: A Regularization Method for Supervised and Semi-Supervised Learning. *IEEE Transactions on Pattern Analysis and Machine Intelligence*, pages 1–16, 2018.
- [31] Volodymyr Mnih, Koray Kavukcuoglu, David Silver, Andrei A Rusu, Joel Veness, Marc G Bellemare, Alex Graves, Martin Riedmiller, Andreas K Fidjeland, Georg Ostrovski, et al. Human-level control through deep reinforcement learning. *Nature*, 518(7540):529–533, 2015.
- [32] Seyed Mohsen Moosavi-Dezfooli, Alhussein Fawzi, and Pascal Frossard. DeepFool: A Simple and Accurate Method to Fool Deep Neural Networks. *Proceedings of the IEEE Computer Society Conference on Computer Vision and Pattern Recognition*, 2016-Decem:2574–2582, 2016.

- [33] Nicolas Papernot, Patrick McDaniel, Ian Goodfellow, Somesh Jha, Z. Berkay Celik, and Ananthram Swami. Practical black-box attacks against machine learning. *ASIA CCS 2017 - Proceedings of the 2017 ACM Asia Conference on Computer and Communications Security*, pages 506–519, 2017.
- [34] Chongli Qin, James Martens, Sven Gowal, Dilip Krishnan, Krishnamurthy Dvijotham, Alhussein Fawzi, Soham De, Robert Stanforth, and Pushmeet Kohli. Adversarial Robustness Through Local Linearization. (NeurIPS):1–10, 2020.
- [35] Jonas Rauber, Wieland Brendel, and Matthias Bethge. Foolbox: A python toolbox to benchmark the robustness of machine learning models. In *Reliable Machine Learning in the Wild Workshop, 34th International Conference on Machine Learning*, 2017.
- [36] Jerome Rony, Luiz G. Hafemann, Luiz S. Oliveira, Ismail Ben Ayed, Robert Sabourin, and Eric Granger. Decoupling direction and norm for efficient gradient-based l2 adversarial attacks and defenses. *Proceedings of the IEEE Computer Society Conference on Computer Vision and Pattern Recognition*, 2019-June:4317–4325, 2019.
- [37] Andrew Slavin Ros and Finale Doshi-Velez. Improving the adversarial robustness and interpretability of deep neural networks by regularizing their input gradients. *32nd AAAI Conference on Artificial Intelligence, AAAI 2018*, pages 1660–1669, 2018.
- [38] Lukas Schott, Jonas Rauber, Matthias Bethge, and Wieland Brendel. Towards the first adversarially robust neural network model on mnist. *arXiv preprint arXiv:1805.09190*, 2018.
- [39] David Silver, Julian Schrittwieser, Karen Simonyan, Ioannis Antonoglou, Aja Huang, Arthur Guez, Thomas Hubert, Lucas Baker, Matthew Lai, Adrian Bolton, et al. Mastering the game of go without human knowledge. *Nature*, 550(7676):354–359, 2017.
- [40] Samrath Sinha, Sayna Ebrahimi, and Trevor Darrell. Variational adversarial active learning. *Proceedings of the IEEE International Conference on Computer Vision*, 2019-Octob:5971–5980, 2019.
- [41] Chawin Sitawarin, Supriyo Chakraborty, and David Wagner. Improving adversarial robustness through progressive hardening. *arXiv preprint arXiv:2003.09347*, 2020.
- [42] Chuanbiao Song, Kun He, Liwei Wang, and John E Hopcroft. Improving the generalization of adversarial training with domain adaptation. In *ICLR*, pages 1–14, 2019.
- [43] Chuanbiao Song, He Kun, Lin Jiadong, John E Hopcroft, and Liwei Wang. Robust local features for improving the generalization of adversarial training. In *ICLR*, pages 1–12, 2020.
- [44] Christian Szegedy, Joan Bruna, Dumitru Erhan, Ian Goodfellow, Joan Bruna, Rob Fergus, and Dumitru Erhan. Intriguing properties of neural networks. pages 1–10.
- [45] Eric Tzeng, Judy Hoffman, Kate Saenko, and Trevor Darrell. Adversarial discriminative domain adaptation. *Proceedings - 30th IEEE Conference on Computer Vision and Pattern Recognition, CVPR 2017*, 2017-January:2962–2971, 2017.
- [46] Oriol Vinyals, Igor Babuschkin, Wojciech M Czarnecki, Michaël Mathieu, Andrew Dudzik, Junyoung Chung, David H Choi, Richard Powell, Timo Ewalds, Petko Georgiev, et al. Grandmaster level in starcraft ii using multi-agent reinforcement learning. *Nature*, 575(7782):350–354, 2019.
- [47] Dongxian Wu, Yisen Wang, and Xia Shu-Tao. Revisiting Loss Landscape for Adversarial Robustness. *ICML*, 2019.
- [48] Cihang Xie and Alan Yuille. Intriguing properties of adversarial training at scale. In *ICLR*, pages 1–14, 2020.
- [49] Daniel L K Yamins, Ha Hong, Charles F Cadieu, Ethan A Solomon, Darren Seibert, and James J DiCarlo. Performance-optimized hierarchical models predict neural responses in higher visual cortex. *Proceedings of the National Academy of Sciences of the United States of America*, 111(23):8619–24, 2014.
- [50] Jihyeon Yoon, Kyungyul Kim, and Jongseong Jang. Propagated perturbation of adversarial attack for well-known CNNs: Empirical study and its explanation. *Proceedings - 2019 International Conference on Computer Vision Workshop, ICCVW 2019*, pages 4226–4234, 2019.
- [51] Runtian Zhai, Chen Dan, Di He, Huan Zhang, Boqing Gong, Pradeep Ravikumar, Cho-Jui Hsieh, and Liwei Wang. Macer: Attack-free and scalable robust training via maximizing certified radius. *arXiv preprint arXiv:2001.02378*, 2020.

- [52] Hongyang Zhang, Yaodong Yu, Jiantao Jiao, Eric P Xing, Laurent El Ghaoui, and Michael I Jordan. Theoretically principled trade-off between robustness and accuracy. *arXiv preprint arXiv:1901.08573*, 2019.
- [53] Huan Zhang, Hongge Chen, Chaowei Xiao, Sven Gowal, Robert Stanforth, Bo Li, Duane Boning, and Cho-Jui Hsieh. Towards Stable and Efficient Training of Verifiably Robust Neural Networks. pages 1–25, 2019.
- [54] Jun-Yan Zhu, Taesung Park, Phillip Isola, and Alexei A Efros. Unpaired image-to-image translation using cycle-consistent adversarial networks. In *Proceedings of the IEEE international conference on computer vision*, pages 2223–2232, 2017.

## 8 Appendix

### 8.1 Network architectures

**MNIST:** We ran our experiments on a shallow ResNet architecture [16] which we called ResNet5. The ResNet5 architecture consists of 1 convolutional layer with stride 2 and 32 filters, a batch normalization layer and ReLU nonlinearity followed by a ResNet block (v1) with stride 2 and 64 filters, global average pool and a ReLU FC layer with 200 units (Table-A1). Activations before the last linear layer were used as high-level network embedding. Objective function was optimized using SGD algorithm with 0.9 momentum.

Table A1: ResNet5 architecture.

Input (1x28x28)
Conv2D (32, stride=2)
BatchNorm2D (32)
ReLU
ResNet Block (64, stride=2)
Global Average Pool (7x7)
FC (200)
ReLU
FC (10)

**CIFAR10 and CIFAR100:** We trained the ResNet18 architecture [16] using SGD optimizer with 0.8 momentum and learning rates as indicated in Table-A2, weight decay of  $10^{-4}$ , batch size of 64, for 850 epochs. All learning rates were reduced by a factor of 10 after epochs 350 and 700.

Table A2: Training hyperparameters for each dataset and network.

Dataset	Model	$\text{LR}_E$	$\text{LR}_{Da}$	$\text{LR}_{EDc}$	weight decay	batch size	Num. Epochs
MNIST	ResNet5	0.5	0.1	0.1	$10^{-4}$	50	300
CIFAR-10	ResNet18	0.5	0.1	0.1	$10^{-4}$	64	850
CIFAR-100	ResNet18	0.5	0.1	0.1	$10^{-4}$	64	850

### 8.2 Adversarial attacks

We used a range of adversarial attacks in our experiments. Hyperparameters associated with each attack are listed in the table below. Implementation of these attacks were adopted from Foolbox [35], AdverTorch [9] packages.

### 8.3 Bound on classifier’s robust error

Considering the embedding distributions in response to clean and perturbed inputs (of a particular class) as two distinct domains of inputs, it is straight forward to use the math from domain adaptation literature to derive a bound on the classifier’s robust error (i.e. under the perturbed scenario). In this case, we can directly adapt *Theorem 2* in [3] to derive this bound.

If  $\mathcal{D}_c$  and  $\mathcal{D}_p$  are distributions of embeddings in response to clean and perturbed inputs of a particular class  $y_i$  respectively. Let  $\mathcal{U}_c$  and  $\mathcal{U}_p$  be samples of size  $m$  each, drawn from  $\mathcal{D}_c$  and  $\mathcal{D}_p$ . Let  $\mathcal{H}$  be a hypothesis space of VC dimension  $d$ , then for any  $\delta \in (0, 1)$ , with probability at least  $1-\delta$  (over the choice of the samples), for every  $h \in \mathcal{H}$ :

$$\epsilon_p(h) \leq \epsilon_c(h) + \frac{1}{2} \hat{d}_{\mathcal{H}\Delta\mathcal{H}}(\mathcal{U}_c, \mathcal{U}_p) + 4\sqrt{\frac{2d\log(2m) + \log(\frac{2}{\delta})}{m}} + \lambda$$

Table A3: Attack hyperparameters for each dataset and attack.

Attack	Dataset	Steps	$\epsilon$	More	Toolbox
FGSM	MNIST	1	$[0, 0.2, 0.3, 0.5, 0.8]$	-	Foolbox
	CIFAR		$[0, \frac{2}{255}, \frac{4}{255}, \frac{8}{255}, \frac{16}{255}, \frac{32}{255}, \frac{64}{255}]$	-	
PGD- $L_1$	MNIST CIFAR	50	$[0, 10, 50, 100, 200, 400]$	step=0.025	Foolbox
PGD- $L_2$	MNIST CIFAR	50	$[0, 2, 5, 10, 20]$	step=0.025	Foolbox
PGD- $L_\infty$	MNIST	40	$[0.0, 0.1, 0.3, 0.5, 0.8, 1]$	step=0.033	Foolbox
	CIFAR	20	$[0, \frac{2}{255}, \frac{4}{255}, \frac{8}{255}, \frac{16}{255}, \frac{32}{255}]$	step= $\frac{2}{255}$	
MIM	MNIST	40	$[0, 0.1, 0.3, 0.5, 0.8, 1]$	-	AdverTorch
	CIFAR		$[0, \frac{2}{255}, \frac{4}{255}, \frac{8}{255}, \frac{16}{255}, \frac{32}{255}]$	-	
DDN	MNIST	100	$[0, 1, 2, 5, 10]$	-	Foolbox
	CIFAR		$[0, 2, 5, 10, 15]$	-	
Deepfool	MNIST	50	$[0, 0.01, 0.1, 0.3, 0.5, 1]$	-	Foolbox
	CIFAR		$[0, \frac{2}{255}, \frac{4}{255}, \frac{8}{255}, \frac{16}{255}, \frac{32}{255}, \frac{64}{255}]$	-	
C&W	MNIST CIFAR	100	$[0, 1, 2, 5]$	stepsize=0.05	Foolbox

where  $\epsilon_c$  and  $\epsilon_p$  are the errors on clean and perturbed inputs,  $\hat{d}_{\mathcal{H}\Delta\mathcal{H}}$  is the empirical  $\mathcal{H}$ -divergence [3], and  $\lambda$  is the combined error of the ideal hypothesis  $h^*$ :  $\lambda = \epsilon_c(h^*) + \epsilon_p(h^*)$ .

Table A4: Comparison of robust performance against Boundary attack [4] with 5000 steps and  $\epsilon = 1$  on different datasets using various methods. We tested the robust performance of each model on 100 random samples from each dataset's test-set.

Dataset	Model	Method	Boundary Attack
MNIST	RN5	NT	6
		AT	98
		TRADES	98
		AFD	95
CIFAR10	RN18	NT	12
		AT	66
		TRADES	72
		AFD	74
CIFAR100	RN18	NT	8
		AT	43
		TRADES	43
		AFD	45

Table A5: Dimensionality of the learned embedding space on various datasets using different methods and measures. Units: number of non-zero embedding dimensions over the test-set within each dataset. Dims: number of PCA dimensions that account for 99% of the embedding variance across all images within the test-set of each dataset.

Dataset	MNIST		CIFAR10		CIFAR100	
Network	RN5		RN18		RN18	
	Units	Dims	Units	Dims	Units	Dims
NT	173	13	512	24	512	431
AT	153	27	512	455	512	481
TRADES	156	52	512	349	512	461
AFD	31	4	380	7	490	88

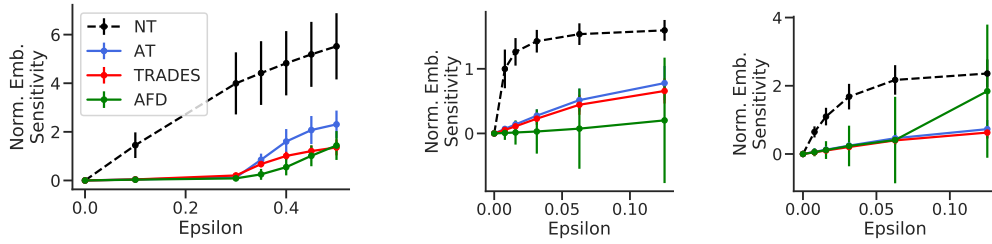


Figure A1: Comparison of normalized embedding sensitivity on test-set of MNIST (left), CIFAR10 (middle), CIFAR100 (right) datasets under PGD- $L_\infty$  attack. For each image, we computed the normalized embedding sensitivity as  $\frac{\|E(x) - E(x')\|_2}{\|E(x)\|_2}$ . Plots show the median sensitivity over test-set of each dataset. Error bars correspond to standard deviation.

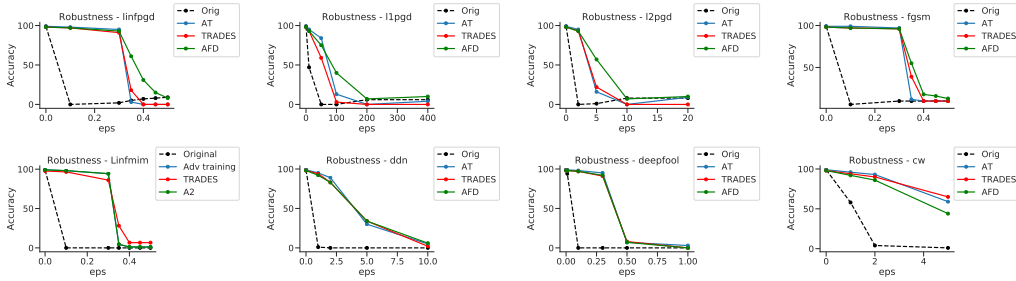


Figure A2: Comparison of robust accuracy of different methods against white-box attacks on MNIST dataset with ResNet5 architecture.

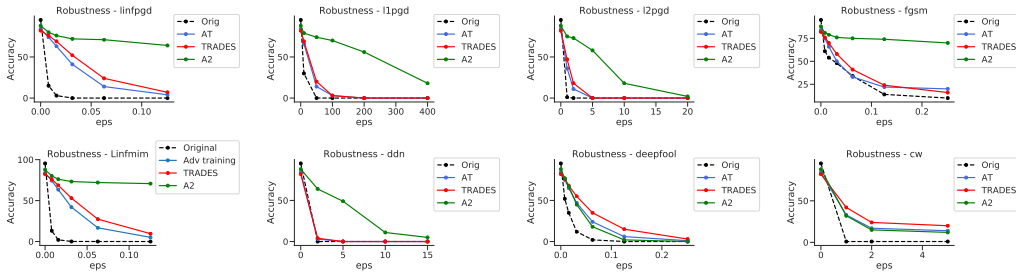


Figure A3: Comparison of robust accuracy of different methods against white-box attacks on CIFAR10 dataset with ResNet18 architecture.

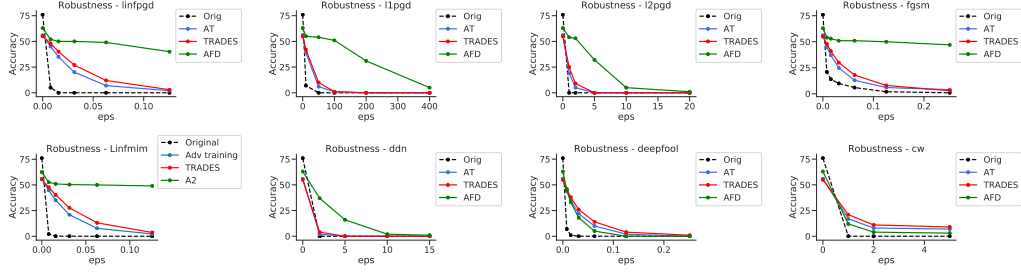


Figure A4: Comparison of robust accuracy of different methods against white-box attacks on CIFAR100 dataset with ResNet18 architecture.

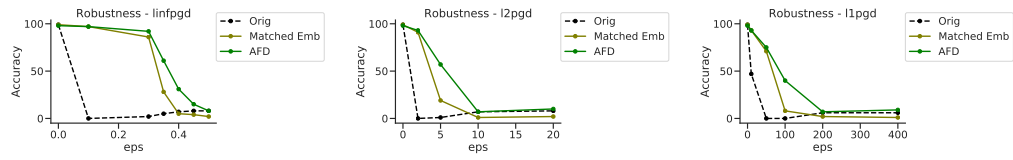


Figure A5: Comparison of robust accuracy of AFD and embedding matching against white-box attacks on MNIST dataset with ResNet5 architecture.



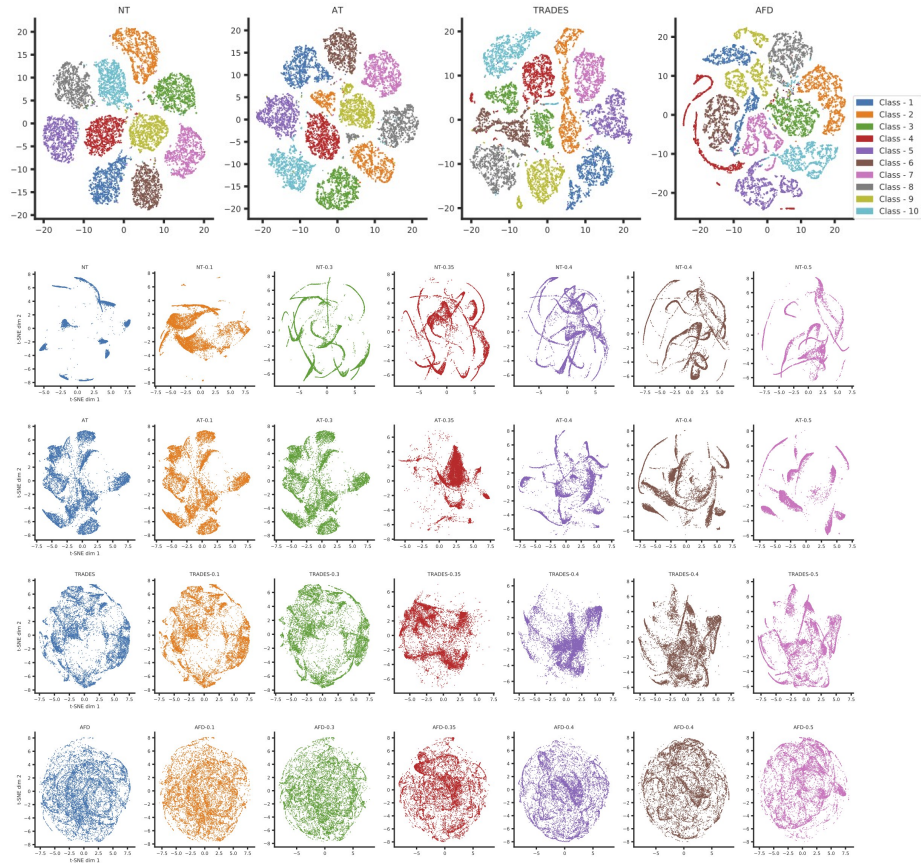


Figure A6: Scatter plot of 2-dimensional t-SNE projection [25] of the embedding derived from training the ResNet5 architecture on MNIST dataset. (top row) t-SNE projection of embeddings of clean images for networks trained with different methods. Each point corresponds to the embedding of one of the images from the MNIST test-set. (rows 2 to 5) t-SNE projection of the embedding of the clean and perturbed MNIST test-set images. Columns are sorted from left to right with the strength of the perturbation (left-most column corresponds to clean images and right-most column with highest tested perturbation). Perturbations are generated using PGD- $L_\infty$  attack. NT: naturally trained; AT: adversarially trained[26]; TRADES: [52]; AFD: adversarial feature desensitization.

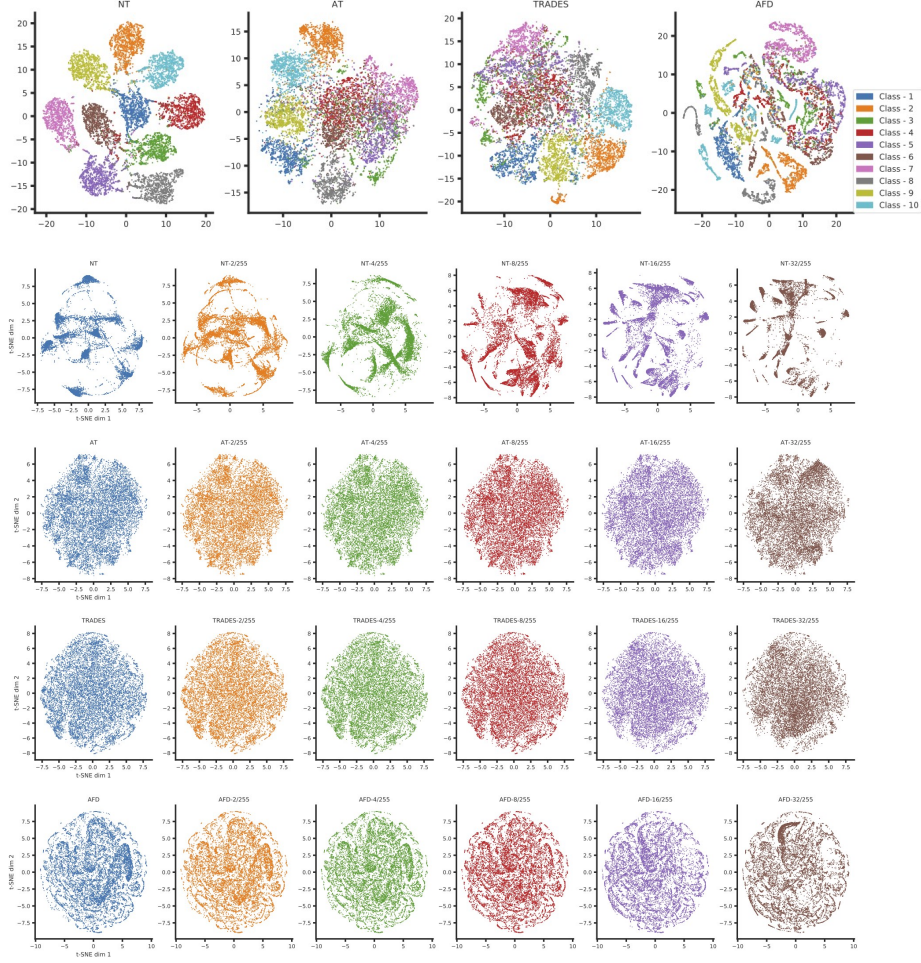


Figure A7: Scatter plot of 2-dimensional t-SNE projection [25] of the embedding derived from training the ResNet5 architecture on CIFAR10 dataset. (top row) t-SNE projection of embeddings of clean images for networks trained with different methods. Each point corresponds to the embedding of one of the images from the CIFAR10 test-set. (rows 2 to 5) t-SNE projection of the embedding of the clean and perturbed CIFAR10 test-set images. Columns are sorted from left to right with the strength of the perturbation (left-most column corresponds to clean images and right-most column with highest tested perturbation). NT: naturally trained; AT: adversarially trained[26]; TRADES: [52]; AFD: adversarial feature desensitization.

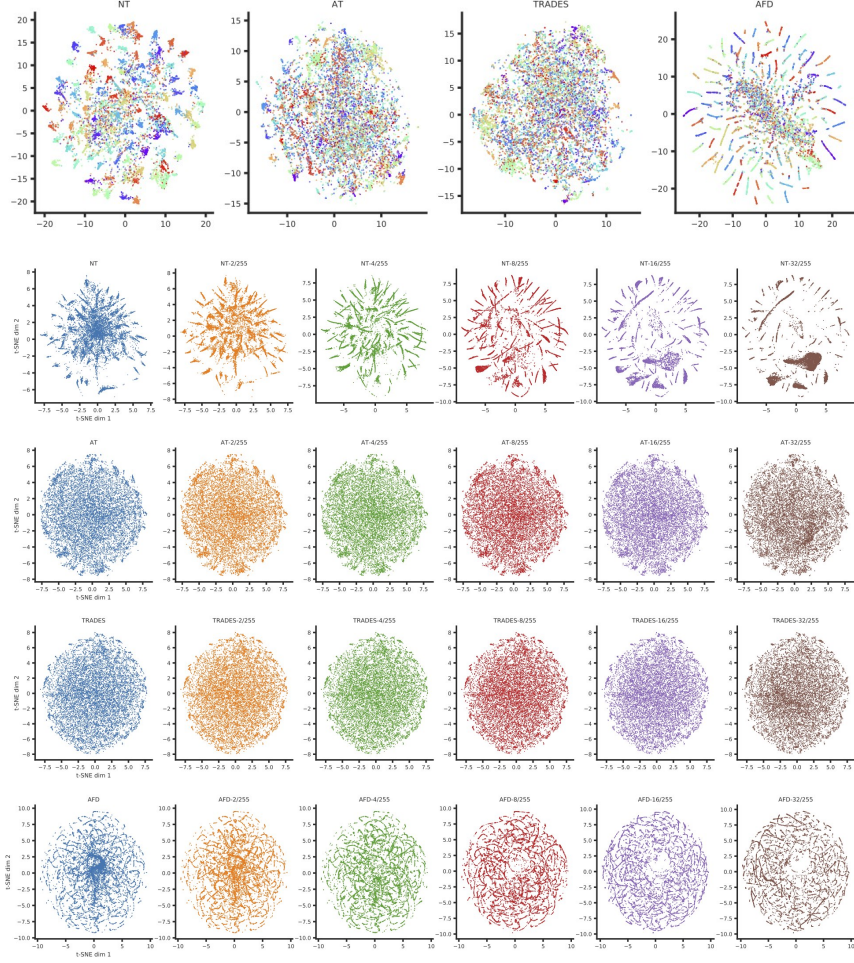


Figure A8: Scatter plot of 2-dimensional t-SNE projection [25] of the embedding derived from training the ResNet5 architecture on CIFAR100 dataset. (top row) t-SNE projection of embeddings of clean images for networks trained with different methods. Each point corresponds to the embedding of one of the images from the CIFAR100 test-set. (rows 2 to 5) t-SNE projection of the embedding of the clean and perturbed CIFAR100 test-set images. Columns are sorted from left to right with the strength of the perturbation (left-most column corresponds to clean images and right-most column with highest tested perturbation). NT: naturally trained; AT: adversarially trained [26]; TRADES [52]; AFD: adversarial feature desensitization.